E2F1 promotes, JNK and DIAP1 inhibit, and chromosomal position has little effect on radiation-induced Loss of Heterozygosity in *Drosophila*

Jeremy Brown[1] and Tin Tin Su[2,3]

Department of Molecular, Cellular and Developmental Biology, 347 UCB,
University of Colorado, Boulder, CO 80309-0347

[1] University of Colorado, Anschutz Medical Campus, 13001 E. 17th Pl., Aurora, CO 80045

[2] University of Colorado Cancer Center, Anschutz Medical Campus, 13001 E. 17th Pl., Aurora, CO 80045

[3]Corresponding author: tin.su@colorado.edu

Short title: Determinants of radiation-induced genome instability

Keywords: *Drosophila*, radiation, loss of heterozygosity

Abstract

Loss of Heterozygosity (LOH) can occur when a heterozygous mutant cell loses the remaining wild type allele to become a homozygous mutant. LOH can have physiological consequences if, for example, the affected gene encodes a tumor suppressor. We used two fluorescent reporters to study mechanisms of LOH induction by X-rays, a type of ionizing radiation (IR), in *Drosophila* larval wing discs. IR is used to treat more than half of cancer patients, so understanding its effects is of biomedical relevance. We report that IR-induced LOH does not correlate with the chromosomal position of the LOH locus, unlike previously shown for spontaneously occurring LOH. Like spontaneous LOH, however, IR-induced LOH of X-linked loci shows a sex-dependence, occurring predominately in females. A focused genetic screen identified E2F1 as a key promotor of LOH and further testing suggests a mechanism involving its role in cell cycle regulation rather than apoptosis. We combined the QF/QS LOH reporter with QUAS-transgenes to manipulate gene function after LOH induction. This approach identified JNK signaling and apoptosis as key determinants of LOH maintenance. These studies reveal previously unknown mechanisms for generation and maintenance of cells with chromosome aberrations after exposure to IR.

36 **Introduction**

37 Loss of Heterozygosity (LOH) occurs when a heterozygous cell loses one of the alleles to
38 become homozygous. LOH can have physiological consequences if, for example, the affected
39 allele encodes a tumor suppressor. Possible mechanisms for the loss of a genetic locus are
40 many and include mutations in the gene, aneuploidy involving loss of whole or segments of
41 chromosomes, and mitotic recombination between the locus and the centromere (producing -
42 /- and +/+ sisters from a -/+ mother cell). We have been using *Drosophila melanogaster* as a
43 model to study LOH that follows exposure to X-rays, a type of ionizing radiation (IR). IR causes
44 single and double strand breaks in the DNA and its ability to induce apoptosis is the reason IR is
45 used to treat half of cancer patients. Understanding IR's effects on genome integrity is a crucial
46 step towards rendering radiation therapy safe by reducing side effects.

47

48 Classical and recent studies of IR-induced LOH in *Drosophila* employed visible adult markers
49 such as *multiple wing hair* (*mwh*) and *forked (f)* that alter the number or morphology of actin-
50 based hairs on the cell surface. Starting with heterozygotes of recessive alleles, induced
51 homozygosity is detected by the presence of mutant hairs and scored on a cell-by-cell basis. In
52 these studies, exposure to IR occurred in the larval stages while the resulting LOH was scored
53 many days later in the adult, with intervening steps poorly understood. To monitor these steps,
54 we have been developing fluorescent reporters for LOH that can be used at all stages of
55 development. We focus our studies on larval wing imaginal discs that develop into the adult
56 wing, the body wall and the hinge that connects the two. Unlike the bulk of the larvae that is
57 made up of polyploid cells that do not undergo mitosis, imaginal discs are comprised of diploid
58 epithelial cells that proliferate by mitotic division.

59

60 In our published work with a fluorescent LOH reporter [1], we used the QF/QS module from the
61 bread mold *Neurospora crassa* wherein QF binds its recognition sequence QUAS to promote
62 transcription while QS represses QF [2]. psc-QF can drive the expression of QUAS-tdTomato
63 (Tom), a fluorescent protein from coral, throughout the wing disc (Fig 1A) unless repressed by
64 ubiquitously-expressed QS^{9B} inserted at 100E1 on chromosome 3 (Fig 1F) [3]. Loss of QS^{9B} by

65 LOH results in de-repression of QF and cell-autonomous Tom expression (Fig 1C-C'). Using this
66 system, we identified two phases of culling of LOH cells, one in late larval stages and another
67 during the pupa stage, that show differential genetic requirements [1].
68
69 Our published study produced two surprising results. First, the incidence of IR-induced LOH as
70 detected by the adult wing marker *mwh* was reproducibly lower by greater than 10-fold when
71 compared to IR-induced LOH detected by QS^{9B} under the same experimental conditions in adult
72 wings [1]. Second, p53, which is required to reduce *mwh* LOH both in our study and others' [1,
73 4], had little effect on QS^{9B} LOH [1]. Classical studies using adult markers suggest a possible
74 explanation. These studies found that 60% of homozygous mutant LOH clones induced by IR
75 lacked a wild type (+/+) twin clone that is expected if mitotic recombination was the
76 mechanism [5]. The same study found that in spontaneously arising LOH clones in un-irradiated
77 animals, 20% of the cells showed a *Minute* bristle phenotype, which is caused by heterozygosity
78 of ribosomal protein loci that are scattered throughout the genome. These data led to the
79 proposal that segmental aneuploidy (loss of a chromosome segment) is the primary mechanism
80 for IR-induced LOH. If breakage and loss of the corresponding chromosome tip is indeed the
81 mechanism, *mwh* LOH would accompany the loss of more genes compared to QS^{9B} LOH
82 because *mwh* is further from the telomere than QS^{9B} (Fig 1F). Resulting *mwh* LOH cells may be
83 less fit than QS^{9B} LOH cells, explaining the difference in IR-induced LOH incidence and p53-
84 dependence we saw. Alternatively, cells that are homozygous mutant for *mwh*, which encodes
85 an actin-bundling protein, may be less fit while the loss of QS, which has no known role in
86 *Drosophila*, may be neutral and it is this difference in gene function that explains the
87 differences in IR-induced LOH incidence and p53-dependence.
88
89 To address these possibilities and to identify regulators of IR-induced LOH, we studied QS^{5A},
90 another QS insertion that is further from the telomere than QS^{9B}, along with five GAL80
91 insertions that span the distance from the telomere to the centromere along the X
92 chromosome (Fig 1F) and performed a focused genetic screen.
93

94 **Results**

95 *Distance from the telomere makes little difference in IR-induced LOH*

96 We used 4000 Rads (R) of X-rays to induce LOH, a dose used by many labs (for example, [6, 7])
97 because it kills more than half of the cells in wing discs by apoptosis, yet most larvae develop
98 into pupae and eclose into viable adults. Thus, this dose of IR causes significant damage but is
99 still compatible with recovery, regeneration, and development. To ask if the distance from the
100 chromosome tip matters, we studied the IR-induced loss of QS^{5A} that is further from the
101 telomere than QS^{9B} or *mwh* (Fig 1F). As we reported for QS^{9B} [1], LOH for QS^{5A} is IR-dependent,
102 with little Tom signal in discs from unirradiated larvae (Fig 2A-B). More important, we saw no
103 statistically significant difference between QS^{9B} and QS^{5A} in terms of IR-induced LOH clone
104 number (Fig 2A) or clone area (Fig 2B). At the developmental stages we study, cells of the wing
105 disc that will ultimately form adult structures are in a single layer columnar epithelium with
106 uniform cell size. Therefore, clone area serves as a proxy for cell number here, as in previous
107 studies [1]. We normalize clone number and area to the total disc area so that we can control
108 for variations in disc size/total cell number. The results suggest that distance from the
109 chromosome tip did not affect LOH incidence.

110

111 Another critical difference we reported between *mwh* and QS^{9B} concerned the role of p53.
112 Using the same RNAi construct and identical experimental conditions to deplete p53, we found
113 that p53 was required to cull cells with *mwh* LOH whereas QS^{9B} LOH was insensitive to p53
114 depletion [1]. We reproduce these findings for QS^{9B} by expressing the same p53 RNAi construct
115 used before or p53 mutants that lack the DNA binding domain and function as dominant
116 negatives [8]. en-GAL4>UAS-GFP marks the posterior (P) compartment where GAL4-driven
117 transgene expression occurs (Fig 1C') while the anterior (A) compartment serves as an internal
118 control. Clone number and area were normalized to compartment area to control for
119 differences in A/P compartment sizes. Transgene expression was initiated with a temperature
120 shift 24h prior to irradiation with 0 R (-IR control) or 4000 R of X-rays, and LOH was quantified
121 after 2 (0 R) or 3 (4000 R) days after irradiation (protocol in Fig 1E). The results confirmed the

122 previous finding that QS^{9B} LOH is insensitive to p53 depletion (Fig 2C-D) and allowed us to test
123 the same on QS^{5A} LOH, which is further from the chromosome tip.
124
125 To assess the sensitivity of QS^{5A} to p53 depletion, we generated a recombinant chromosome 2
126 that bears QS^{5A}, psc-QF>Tom, and en-GAL4>UAS-GFP (this was not needed for QS^{9B} which is on
127 chromosome 3). We characterized ten independent recombinant QS^{5A} lines and found that they
128 consistently produced lower LOH than the parental QS^{5A} (data for two recombinants shown in
129 Fig 2A-B). Perhaps chromosome rearrangements that occurred during recombination interfered
130 with QS^{5A} or psc>Tom expression. More importantly, two recombinant lines with highest level
131 of IR-induced LOH showed no change upon p53 depletion (Fig 2C-D). Collectively, these data
132 suggest that (1) LOH incidence does not correlate with the distance from the telomere and that
133 (2) not all LOH events are sensitive to p53. We speculate that p53 may respond to LOH events
134 differently depending on their consequence on cellular physiology, which is a new idea (see
135 Discussion).
136
137 *IR-induced LOH shows sex-dependence and locus-independence*
138 To more rigorously test the idea that IR-induced LOH is not dependent on chromosomal
139 position, we turned to a published GAL4/GAL80 system with GAL80 inserted at 5 different
140 locations along the X chromosome that has been used to detect spontaneous (without IR) LOH
141 (Fig 1B,D,F) [9]. For four of the five insertions, wing discs from un-irradiated larvae show very
142 few cells with GFP signal that is as bright as what is seen after IR (Fig 3A-B, Supplemental Fig 1).
143 Occasional cells with faint GFP (arrow in Supplemental Fig 1A-A'') are consistent with a recent
144 report of spontaneous GAL80 'loss' in larval brains through poorly understood mechanisms
145 [10]. Importantly, we noticed in early experiments with GAL80 that approximately half of the
146 irradiated discs lacked GFP expressing clones. This is different from what we saw with QS, for
147 example, 32 of 38 QS^{9B} discs had Tom+ cells in Fig 2A '9B+IR' dataset. QS insertions are on
148 autosomes while GAL80 insertions are on the X chromosome. This led us to hypothesize a sex-
149 dependence in GAL80 LOH, similar to what was reported previously for spontaneous LOH of X-
150 linked loci [9]. To address this possibility, we separated males and female larvae before

151 dissection and found that IR-induced increases in GFP+ cells were confined almost exclusively to
152 females (Fig 3C-D).
153
154 The exception is the 12C6 insertion, which shows the greatest incidence of GFP+ cells without
155 IR via unknown mechanisms, and a further increase after IR (Fig 3E-F). Even in this case, IR
156 induced increase was significant only in the females (Fig 3G-J, quantified in E and F). Thus, IR-
157 induced GAL80 LOH shows a sex-dependence for all five insertions, similar to the case for
158 spontaneous LOH [9]. To our surprise, however, IR-induced LOH in terms of clone number or
159 clone area did not decrease with proximity to the centromere (Fig 3C-D). This is unlike what was
160 observed before for spontaneous LOH, which decreased with increasing proximity to the
161 centromere for both X and autosomal loci [9]; $GAL80^{5B}$ showed spontaneous LOH in 75% of
162 adult *Drosophila* intestines while the same parameter for $GAL80^{19E}$ was 40%. In contrast, IR-
163 induced LOH clone number and area were nearly identical for $GAL80^{5B}$ and $GAL80^{19E}$ (Fig 3C-D,
164 p=0.193 for clone number and 0.861 for clone area). We conclude that IR-induced LOH shows
165 sex-dependence but chromosomal position independence. Possible explanations for these
166 results are provided in the Discussion.
167
168 *A focused screen identified E2F1 as a regulator of LOH*
169 Results so far address cis-acting determinants, namely, chromosome position of the LOH loci
170 and the presence of a homologous X chromosome. To identify trans-acting regulators of LOH,
171 we performed a focused screen through known regulators of DNA damage and stress
172 responses, cell growth, cell survival and cell competition (see Supplemental Table 1 for the full
173 list), using published constructs that have been shown to produce a phenotype, when possible.
174 We used QS rather than GAL80 in this screen so that we can use the GAL4/UAS system in
175 parallel to knock down/overexpress genes. We used QS^{9B} rather than QS^{5A} because the former
176 shows more robust IR-induced LOH incidence.
177
178 Genes were knocked down or over-expressed in the posterior (P) half of wing discs using the
179 protocol in Fig 1E. As stated above, we saw no Tom clones without IR; therefore, only +IR data

180 are shown (Fig 4 and Supplemental Fig 2). Three controls were used: the parental TRiP III line
181 that was the recipient of many RNAi constructs and RNAi for the w gene (both as controls for
182 RNAi) and w^{1118} (control for overexpression or OE). IR-induced LOH clone number or area are
183 not significantly different between A and P compartments in all three controls (Fig 4A-B and
184 Supplemental Fig 2). Most of the genes tested did not alter IR-induced LOH significantly
185 (Supplemental Fig 2), including those with known roles in cell competition such as duox,
186 Myo31D and Xrp1. This group is of interest because a prior publication suggested that cells with
187 segmental aneuploidy, a possible mechanism for LOH generation, may be eliminated by cell
188 competition [11]. We interpret negative results with caution, however, because our protocol
189 for conditional and transient expression (Fig 1E) may not deplete gene function sufficiently
190 even if the same construct produced a phenotype under different expression conditions before.
191
192 The screen found mild effects with RNAi against Chk2 or Myc and with overexpression of
193 oncogenic Ras^{V12} (Fig 4A-B). Specifically, Chk2 RNAi increased LOH clone number while Myc
194 RNAi and Ras^{V12} decreased LOH clone number. The effect sizes, however, were small (1.5 to 2-
195 fold) and clone area was not significantly affected, suggesting compensating changes in the size
196 of individual clones. In addition, expressing Ras^{V12} in the P compartment, we found, produced
197 epithelial folds in both P and A compartments in irradiated discs (Fig 4D-D'), making the
198 quantification of clone area challenging. Because of this and small effect sizes, we have not
199 followed up on Chk2, Myc and Ras further.
200
201 In contrast, we observed a profound effect on both LOH clone number and clone area with
202 RNAi against E2F1, a reduction of the former by 6-fold and the latter by more than 10-fold (Fig
203 4C, quantified in A-B). *Drosophila* E2F1, like its mammalian homologs, functions in cell cycle
204 regulation where it promotes G1/S transition via activation of cyclin E expression and G2/M
205 transition via activation of String (*Drosophila* Cdc25) [12]. It is also known to promote IR-
206 induced apoptosis in the wing discs when p53 has been depleted; that is, its role in IR-induced
207 apoptosis is negligible in a wild type background [13]. Therefore, we addressed the more likely
208 possibility that the requirement for E2F1 in LOH clone formation/maintenance is through its

209 role in the cell cycle. To this end, we expressed Cdk inhibitors Dap and Rux to inhibit G1/S and
210 G2/M transitions, respectively, using the same temperature shift protocol as in Fig 1E. Both Dap
211 and Rux phenocopied E2F1 RNAi (Fig 4A-B), supporting the idea that the role of E2F1 is to
212 promote the proliferation of cells with LOH.
213
214 As explained above, we normalize LOH clone number and LOH area to the area of the
215 compartment. If E2F1 RNAi or overexpression of Dap and Rux in the P compartment affected all
216 cells within this compartment equally regardless of their LOH status, we should see little change
217 in normalized LOH clone number or area. Yet, we see multiple-fold reductions by both
218 measures. We infer that manipulations of cell cycle regulators have a more severe effect on
219 cells with LOH than on cells in the rest of the P compartment. Greater sensitivity of LOH cells to
220 cell cycle inhibition is a new finding.
221
222 The manipulations thus far alter gene expression in the whole compartment and identified
223 differential effects on LOH versus non-LOH cells. To address cell-autonomous needs in LOH cells
224 more directly, we took advantage of QS loss and consequent QF de-repression to express
225 QUAS-transgenes and assayed their effect. This protocol has the added advantage of identifying
226 needs AFTER the clones have formed and have initiated QF-mediated gene expression. As
227 proof-of-concept, we used a published QUAS-rpr transgene [14] to express this pro-apoptotic
228 gene specifically in LOH clones, with the expectation that such clones will be lost to cell death.
229 The results show that the system works as expected; the addition of QUAS-rpr reduced both
230 clone number and clone area to near completion (Fig 5A-B, quantified in E-F).
231
232 Using QUAS-transgenes to express inhibitors, we tested the role of JNK and apoptotic signaling
233 in maintaining cells with LOH. We first assessed the functionality of each transgene by
234 expressing them ubiquitously with the psc-QF promoter (without QS) and assaying for expected
235 phenotypes. For rpr, dominant negative bsk (*Drosophila* JNK) and puc (phosphatase and JNK
236 inhibitor), we were able to identify lines that produced significant lethality (Supplemental Table
237 2). For *Drosophila* Inhibitor of Apoptosis Protein 1 (DIAP1), even the strongest and statistically

238 significant effect on lethality was modest. Therefore, we assayed for inhibition of apoptosis
239 instead. Of three lines tested, QUAS-DIAP1 12M reduced IR-induced cleaved Dcp1 signal to near
240 completion (Fig 5H), 14F showed a modest effect (Fig 5I), and 3M showed variable effect from
241 disc to disc. Therefore, QUAS-DIAP1 12M line was used in subsequent experiments. The results
242 show that LOH cell-autonomous inhibition of JNK or apoptosis led to a significant increase in
243 both Tom clone number and area. We conclude that in cells that survived LOH long enough to
244 activate QF-mediated transgene expression, stress signaling continues to operate to eliminate
245 them.
246
247 **Discussion**
248 We report here studies on the role of chromosomal position and trans-acting regulators on IR-
249 induced LOH in *Drosophila* larval wing discs. We found that position along the chromosome
250 makes little difference while the presence of a homologous chromosome is required. We
251 identified E2F1 as a positive regulator of LOH clone incidence and propose that cells with LOH
252 are more sensitive to inhibition of cell proliferation than their neighbors. And we identified JNK
253 signaling and apoptosis as cell-autonomous mechanisms that eliminate cells that survived LOH
254 induction.
255
256 Spontaneous LOH in the adult *Drosophila* intestine is attributed to mitotic recombination,
257 based on several lines of evidence. First, sex-dependence is interpreted as arising from
258 recombination-based mechanisms that require the presence of a homologous chromosome
259 such as crossing over, gene conversion or break-Induced replication [9]. Second, adult guts with
260 spontaneous GAL80^{5B} LOH was about twice as frequent as those with spontaneous GAL80^{19E}
261 LOH. An increase in LOH with distance from the centromere is predicted for recombination-
262 based mechanisms because a distal locus would experience more frequent exchanges between
263 homologous chromosomes. This study noted, however, that the frequency of spontaneous LOH
264 at 19E was higher than predicted from meiotic maps and higher than observed for a
265 centromere-proximal locus on chromosome 3R, suggesting additional factors at play. Third,

266 whole genome sequencing confirmed that spontaneous LOH of chromosome 2 loci in the adult
267 intestine occur through mitotic recombination [15].
268
269 Our finding that IR-induced LOH clone number and area were nearly identical for GAL80^{5B} and
270 GAL80^{19E} cannot be explained by recombination-based mechanisms. Classical studies by Baker
271 and others monitored several adult visible markers such as *yellow (y)* and *forked (f)* in
272 heterozygous adult females that were irradiated as larvae or pupae with 1000 R from a Co-60
273 source [5]. In adult female abdomens monitored for *y* or *f*, both X-linked genes, 40% of LOH
274 clones induced by IR (i.e., the difference between -/+IR samples) consisted of 40% twin clones
275 (likely products of mitotic recombination) and the remaining 60% were single clones.
276 Examination of single clones that arose spontaneously (without radiation) in the same study
277 found that 20% of cells in such clones showed *Minute* bristles, which result from
278 haploinsufficiency of loci encoding ribosomal proteins. The authors suggest that single LOH
279 clones arose by aneuploidy that turned wild type (+/+) cells into heterozygotes for ribosomal
280 protein genes (M/+). In another set of studies, McNamee and Brodsky used the *Minute* bristle
281 phenotype and assayed gain-of-heterozygosity, from +/+ to M/+, rather than loss-of-
282 heterozygosity, in bristles from adults that result from irradiated larvae [11]. Recombination-
283 based mechanisms induced by IR would not be detectable in this assay as it would change +/+
284 to +/+. Regardless, taken together, these results suggest that both aneuploidy and
285 recombination-based mechanisms operate to produce IR-induced LOH in tissues that produce
286 the adult body wall. Our data suggest a greater contribution by non-recombination-based
287 mechanisms.
288
289 How then do we explain our finding that LOH of X-linked loci requires a homologous
290 chromosome? We suggest that without part or whole of the X chromosome in XY males, a cell
291 may not survive to express GFP, reducing the level of LOH observed in males. In other words,
292 presence of one X chromosome allows cells to survive with partial or complete loss of the other
293 X chromosome. The results of studies by Baker, Brodsky and colleagues did not distinguish
294 among various types of aneuploidy, which can include whole chromosome loss, segmental

295 aneuploidy (loss of a chromosomal segment) and terminal deletions, as specific mechanisms for
296 IR-induced genomic rearrangements. Over-expression of telomere capping protein HipHop has
297 been shown to increase the survival of cells with terminal deletions that result from dividing
298 experimentally induced dicentric chromosomes [16]. Overexpression of HipHop, however, did
299 not increase the incidence of IR-induced LOH (Supplemental Fig 2), suggesting that terminal
300 deletions may not be the mechanism. The finding that distance from the telomere did not
301 affect the QS LOH incidence supports this idea. Instead, relevant types of aneuploidy may
302 include X-ray-induced segmental losses that are well-documented in numerous studies in
303 *Drosophila* and mammals (for example, [17-20]).
304
305 McNamee and Brodsky found that p53 single mutants, *hid* single mutants, and p53 *hid* double
306 mutants show progressively higher incidence of IR-induced *Minute* (M/+) bristles, in that order
307 [11]. The authors interpreted the data to mean that while p53 makes a partial contribution to
308 removing M/+ cells, there is also a p53-independent mechanism and that *hid* is involved in
309 both. Additional data implicate JNK signaling in activating *hid* but only when p53 is absent. In
310 other words, p53 and JNK play primary and back-up roles, respectively, in eliminating cells with
311 chromosome aberrations that affect the Minute loci. In contrast, we detect a minimal effect of
312 p53 depletion and a significant effect of JNK inhibition (even when p53 is wild type) on QS LOH
313 (this study), and a significant effect of p53 depletion on *mwh* LOH [1]. We propose that the
314 effect of p53 on cells with LOH depends on whether the LOH affects the fitness of cells (*mwh*
315 and M) or not (QS and GAL80). The requirement for JNK may be the reverse because we detect
316 a need for it in repressing the less deleterious QS LOH (this study) while it plays a secondary
317 role to p53 in culling M/+ cells that experience a lowered fitness [11].
318
319 **Materials and Methods**
320 *Drosophila stocks and methods*
321 *Drosophila* stocks used in this work are listed in Supplemental Table 1 and include UAS-puc [21],
322 UAS-Wg [22], and stocks bearing recombinant chromosome 2 of the genotype psc-QF, QUAS-
323 Tom, en-GAL4, UAS-GFP, tub-QS^{5A} balanced over CyO-GFP and recombinant chromosome 3 of

324 the genotype tub-QS^{9B}, tub-GAL80^{ts} [1]. Virgin females and males were crossed and cultured for
325 three days on Nutri-Fly German Formula food (Genesee Scientific) at 25°C before egg
326 collections.
327
328 *Larvae culture and irradiation*
329 Eggs were collected and larvae were raised on Nutri-Fly Bloomington Formula food (Genesee
330 Scientific) at 25°C unless otherwise noted. The cultures were monitored daily for signs of
331 crowding, typically seen as 'dimples' in the food surface as larvae try to increase the surface
332 area for access to air. Cultures were split at the first sign of crowding. Larvae in food were
333 placed in petri dishes and irradiated in a Faxitron Cabinet X-ray System Model RX-650
334 (Lincolnshire, IL) at 115 kVp and 5.33 rad/sec. Larval sex was determined using gonad size
335 observed under a dissecting microscope; males have large, clearly visible gonads free of the fat
336 body while female gonads are hard to find [23]. For eclosion (Supplemental Table 2), empty and
337 full pupal cases were counted 12-14 days after collection.
338
339 *Tissue preparation and imaging*
340 Larval wing discs were dissected in PBS, fixed in 4% para-formaldehyde (PFA) in PBS for 30 min,
341 and washed three times with PBTx (0.1% Triton X-100). The discs were stained with 10 μg/ml
342 Hoechst33342 in PBTx for 5 min, washed 3 times, and mounted on glass slides in Fluoromount
343 G (SouthernBiotech). Wing discs were imaged on a Leica DMR compound microscope using a Q-
344 Imaging R6 CCD camera and Ocular or Micro-Manager software.
345
346 *Lethality test with QUAS lines*
347 QUAS lines are a kind gift from Ainhoa Pérez-Garijo and Hermann Steller [14]. For insertions on
348 chromosome 2, CyO balancer was floating so CyO+ males were sorted and used. Male QUAS
349 flies were crossed to virgins of the genotype psc-QF>UAS-Tomato/CyO-GFP. Embryos were
350 collected overnight. CyO and CyO+ progenies were counted until no new adults eclosed for a 24
351 h period. X^2 test was used to assess deviations from the 1:1 expected Mendelian ratio. For
352 insertions on chromosome 3, Tb+ pupae were sorted and scored as GFP+ or GFP- before

353 eclosion was monitored. X^2 test was used to assess deviations from the 2GFP- (Sco/QF>Tom
354 and QF>Tom/CyO):1GFP+ (Sco/CyO-GFP) expected Mendelian ratio (See Supplemental Table 2
355 for genotypes of the crosses).
356
357 *Statistical Analysis*
358 For sample size justifications, we used a simplified resource equation from [24]; E = total
359 number of animals − total number of groups, where E value of 10-20 is considered adequate.
360 When we compare two groups (-IR and +IR, for example, where the former is the control group
361 and the latter is the treated group), n = 6 per group, or E = 11, would be adequate. All samples
362 subjected to statistical analysis meet or exceed this criterion. To compute p-values, 2-tailed
363 Student t-tests were used.
364
365 **Acknowledgments**
366 We thank Alison Bardin and Herman Steller for GAL80 and QUAS stocks, respectively. Additional
367 stocks from the Bloomington *Drosophila* Stock Center (NIH P40OD018537) and Vienna
368 *Drosophila* Resource Center were used in this study.
369
370 **Funding**
371 This work was supported by the National Institutes of Health (grant R35 GM130374 to TTS).
372
373

374 **Figure and Table Legends**

375

376 **Fig 1. Fluorescent reporters for loss-of-heterozygosity**

377 A. Loss of QS results in de-repression of psc-QF-driven Tom expression.

378 B. Loss of GAL80 results in de-repression of act-GAL4-driven GFP expression.

379 C-C'. An example of a wing disc with a Tom clone. This disc also expresses en-GAL4>GFP
380 that was used to express RNAi and transgenes in the posterior compartment of the disc. The
381 genotype was en-GAL4>UAS-GFP, psc-QF>Tom, QS^{5A}/+ from the cross of en-GAL4>UAS-GFP,
382 psc-QF>Tom, QS^{5A}/CyO-GFP with w^{1118}. Larvae were treated as in panel E but without the
383 temperature shift.

384 D. An example of a wing disc with GFP clones. The genotype was $GAL80^{5B}$/+; Act-GAL4,
385 UAS-GFP/+ from the cross of $GAL80^{5B}$/$GAL80^{5B}$ with Act-GAL4, UAS-GFP/CyO RFP Tb. Larvae
386 were treated as in panel E but without the temperature shift.

387 E. The experimental protocol used to express RNAi and transgenes conditionally in the
388 focused screen. For experiments that do not involve transgene expression, the same protocol
389 was followed but larvae were maintained at 25°C without a temperature shift.

390 F. Chromosomal location of QS^{5A}, QS^{9B}, *mwh* and GAL80 studied here (not to scale).

391 Scale bar = 120 microns in C-D.

392

393 **Fig 2. Distance from the telomere makes little difference in LOH incidence**

394 Larvae were treated as in Fig 1E but without the temperature shift and wing discs were fixed
395 and stained for DNA. The graphs show data are from at least two biological replicates per
396 sample, with the total number of wing discs examined for each sample is shown in parentheses.
397 Error bars represent mean±1 SEM.

398 (A-B) IR-induced LOH incidence for QS^{9B} and QS^{5A} are not significantly different but two
399 recombinant QS^{5A} lines show reduced LOH compared to parental QS^{5A}. Larvae were treated as
400 in Fig 1E but without the temperature shift. p-values were calculated using a 2-tailed t-test.

401 (C-D) Knocking down of p53 did not affect QS LOH. Larvae were treated as in Fig 1E. p-
402 values were calculated using a paired 2-tailed t-test.

403

404 The genotypes are as shown below. Stock information is in Supplemental Table 1.

405 A-B: 9B = psc-QF>Tom/+; QS^{9B}/+ that results from psc-QF>Tom; QS^{9B} X to w^{1118}

406 5A = psc-QF>Tom/QS^{5A} that results from psc-QF>Tom/CyO-GFP X QS^{5A}/CyO-GFP

407 5A #6 or #11 = en-GAL4>UAS-GFP, psc-QF>Tom, QS^{5A}/+ from the cross of en-GAL4>UAS-

408 GFP, psc-QF>Tom, QS^{5A}/CyO-GFP with w^{1118}

409 C-D: 9B p53 RNAi = UAS-Dcr/+; en>GFP, UAS-$p53^{RNAi}$/psc-QF>Tom; QS^{9B}, $GAL80^{ts}$/+

410 9B p53 H159N or R115H = en>GFP, psc-QF>Tom/+; QS^{9B}, $GAL80^{ts}$/UAS-$p53^{H159N\ or\ R115H}$

411 5A p53 RNAi = UAS-Dcr/+; en>GFP, UAS-$p53^{RNAi}$/psc-QF>Tom, en>GFP, QS^{5A}; $GAL80^{ts}$/+

412

413 **Fig 3. IR-induced LOH shows sex-dependence and locus-independence**

414 Larvae were treated as in Fig 1E but without the temperature shift and wing discs were fixed

415 and stained for DNA. The genotype of the larvae was GAL80/+; Act-GAL4, UAS-GFP/+ from the

416 cross of GAL80/GAL80 with Act-GAL4, UAS-GFP/CyO RFP Tb. The graphs show data from at least

417 two biological replicates per sample, with the total number of wing discs examined per sample

418 shown in parentheses. The mean±1 SEM is shown for each sample. p-values were calculated

419 using a 2-tailed t-test.

420 (A-D) Quantification of GFP+ clone number (A-B) and clone area (C-D) with and without

421 irradiation for four GAL80 insertions on the X chromosome. Male and female larvae were

422 separated before dissection and processed separately.

423 (E-F) Quantification of GFP+ clone number (E) and clone area (F) with and without

424 irradiation for 12C6 GAL80 insertion on the X chromosome. Male and female larvae were

425 separated before dissection and processed separately.

426 (G-J) Representative examples of wing discs for the 12C insertion. Scale bar = 120

427 microns.

428

429 **Fig 4. A focused screen identified E2F1 as a regulator of LOH**

430 Wing discs from 3rd instar larvae were dissected 3 days after irradiation, fixed and stained for

431 DNA. Larvae were treated as in Fig 1E. The graphs show data from at least two biological

432 replicates per sample, with the total number of wing discs examined per sample shown in
433 parentheses. The mean±1 SEM is shown for each sample. p-values were calculated using a
434 paired 2-tailed t-test.
435 (A-B) Results of the focused screen showing clone number (A) and clone area (B). RNAi
436 against w is shown as the control for RNAi constructs and w^{1118} is shown as the control for
437 overexpression constructs.
438 (C-D') Representative examples of wing discs expressing $E2F1^{RNAi}$ or RAS^{V12} in the P
439 compartment (GFP+).
440
441 **Fig 5. Cell autonomous requirements for LOH**
442 (A-D) Larvae were treated as in Fig 1E but without the temperature shift and wing discs
443 were fixed and stained to visualize DNA. The discs shown are from irradiated larvae.
444 (E-F) Quantification of Tom+ clone number (E) and clone area (F) in irradiated discs. The
445 graphs show data from at least two biological replicates per sample, with the total number of
446 wing discs examined per sample shown in parentheses. The mean±1 SEM is shown for each
447 sample. p-values relative to w^{1118} controls were calculated using a 2-tailed t-test.
448 (G-I) Larvae were cultured and irradiated as in (A-F) but wing discs were dissected 4h
449 after IR, fixed and stained for DNA and with an antibody against cleaved active Dcp1 as a
450 surrogate marker for apoptosis.
451 Scale bars = 120 microns.
452 The genotypes are as shown below. Stock information is in Supplemental Table 1.
453 (A,G) Control = psc-QF>Tom/+; QS^{9B}/+ that results from psc-QF>Tom; QS^{9B} X to w^{1118}
454 (H-I) psc-QF>Tom/QUAS-transgene; QS^{9B}/+
455 (B-D) psc-QF>Tom/+; QS^{9B}/QUAS-transgene
456

457 **References**

458 1. Brown J, Bush I, Bozon J, Su TT. Cells with loss-of-heterozygosity after exposure to
459 ionizing radiation in Drosophila are culled by p53-dependent and p53-independent
460 mechanisms. PLoS Genet. 2020;16(10):e1009056. Epub 2020/10/20. doi:
461 10.1371/journal.pgen.1009056. PubMed PMID: 33075096; PubMed Central PMCID:
462 PMCPMC7595702.
463 2. Riabinina O, Luginbuhl D, Marr E, Liu S, Wu MN, Luo L, et al. Improved and expanded Q-
464 system reagents for genetic manipulations. Nat Methods. 2015;12(3):219-22, 5 p following 22.
465 Epub 2015/01/13. doi: 10.1038/nmeth.3250. PubMed PMID: 25581800; PubMed Central
466 PMCID: PMCPMC4344399.
467 3. Potter CJ, Tasic B, Russler EV, Liang L, Luo L. The Q system: a repressible binary system
468 for transgene expression, lineage tracing, and mosaic analysis. Cell. 2010;141(3):536-48. Epub
469 2010/05/04. doi: 10.1016/j.cell.2010.02.025. PubMed PMID: 20434990; PubMed Central
470 PMCID: PMCPMC2883883.
471 4. Sogame N, Kim M, Abrams JM. Drosophila p53 preserves genomic stability by regulating
472 cell death. Proc Natl Acad Sci U S A. 2003;100(8):4696-701. Epub 2003/04/04. doi:
473 10.1073/pnas.0736384100. PubMed PMID: 12672954; PubMed Central PMCID:
474 PMCPMC153618.
475 5. Baker BS, Carpenter AT, Ripoll P. The Utilization during Mitotic Cell Division of Loci
476 Controlling Meiotic Recombination and Disjunction in DROSOPHILA MELANOGASTER. Genetics.
477 1978;90(3):531-78. Epub 1978/11/01. PubMed PMID: 17248870; PubMed Central PMCID:
478 PMCPMC1213905.
479 6. Brodsky MH, Weinert BT, Tsang G, Rong YS, McGinnis NM, Golic KG, et al. Drosophila
480 melanogaster MNK/Chk2 and p53 regulate multiple DNA repair and apoptotic pathways
481 following DNA damage. Mol Cell Biol. 2004;24(3):1219-31. Epub 2004/01/20. doi:
482 10.1128/mcb.24.3.1219-1231.2004. PubMed PMID: 14729967; PubMed Central PMCID:
483 PMCPMC321428.
484 7. Wells BS, Johnston LA. Maintenance of imaginal disc plasticity and regenerative
485 potential in Drosophila by p53. Dev Biol. 2012;361(2):263-76. Epub 2011/11/01. doi:

486 10.1016/j.ydbio.2011.10.012. PubMed PMID: 22036477; PubMed Central PMCID:
487 PMCPMC3296280.
488 8. Ollmann M, Young LM, Di Como CJ, Karim F, Belvin M, Robertson S, et al. Drosophila p53
489 is a structural and functional homolog of the tumor suppressor p53. Cell. 2000;101(1):91-101.
490 Epub 2000/04/25. doi: 10.1016/S0092-8674(00)80626-1. PubMed PMID: 10778859.
491 9. Siudeja K, Nassari S, Gervais L, Skorski P, Lameiras S, Stolfa D, et al. Frequent Somatic
492 Mutation in Adult Intestinal Stem Cells Drives Neoplasia and Genetic Mosaicism during Aging.
493 Cell Stem Cell. 2015;17(6):663-74. Epub 2015/11/27. doi: 10.1016/j.stem.2015.09.016. PubMed
494 PMID: 26607382; PubMed Central PMCID: PMCPMC5138153.
495 10. Goupil A, Heinen JP, Salame R, Rossi F, Reina J, Pennetier C, et al. Illuminati: a form of
496 gene expression plasticity in Drosophila neural stem cells. Development. 2022;149(22). Epub
497 2022/11/19. doi: 10.1242/dev.200808. PubMed PMID: 36399062; PubMed Central PMCID:
498 PMCPMC9845751.
499 11. McNamee LM, Brodsky MH. p53-independent apoptosis limits DNA damage-induced
500 aneuploidy. Genetics. 2009;182(2):423-35. Epub 2009/04/15. doi:
501 10.1534/genetics.109.102327. PubMed PMID: 19364807; PubMed Central PMCID:
502 PMCPMC2691752.
503 12. Reis T, Edgar BA. Negative regulation of dE2F1 by cyclin-dependent kinases controls cell
504 cycle timing. Cell. 2004;117(2):253-64. Epub 2004/04/16. doi: 10.1016/s0092-8674(04)00247-8.
505 PubMed PMID: 15084262.
506 13. Wichmann A, Jaklevic B, Su TT. Ionizing radiation induces caspase-dependent but Chk2-
507 and p53-independent cell death in Drosophila melanogaster. Proc Natl Acad Sci U S A.
508 2006;103(26):9952-7. doi: 10.1073/pnas.0510528103. PubMed PMID: 16785441; PubMed
509 Central PMCID: PMCPMC1502560.
510 14. Perez-Garijo A, Fuchs Y, Steller H. Apoptotic cells can induce non-autonomous apoptosis
511 through the TNF pathway. Elife. 2013;2:e01004. Epub 2013/09/26. doi: 10.7554/eLife.01004.
512 PubMed PMID: 24066226; PubMed Central PMCID: PMCPMC3779319.
513 15. zouabi LA, Stefanutti M, Riddiford N, Rubanova N, Bohec M, Servant N, et al. Molecular
514 Underpinnings and Environmental Drivers of Spontaneous Loss of Heterozygosity in

515 Drosophila Intestinal Stem Cells. bioRxiv. 2022:2022.07.21.500951. doi:
516 10.1101/2022.07.21.500951.
517 16. Kurzhals RL, Fanti L, Ebsen ACG, Rong YS, Pimpinelli S, Golic KG. Chromosome Healing Is
518 Promoted by the Telomere Cap Component Hiphop in Drosophila. Genetics. 2017;207(3):949-
519 59. Epub 2017/09/25. doi: 10.1534/genetics.117.300317. PubMed PMID: 28942425; PubMed
520 Central PMCID: PMCPMC5676247.
521 17. Chick WS, Mentzer SE, Carpenter DA, Rinchik EM, Johnson D, You Y. X-ray-induced
522 deletion complexes in embryonic stem cells on mouse chromosome 15. Mamm Genome.
523 2005;16(9):661-71. Epub 2005/10/26. doi: 10.1007/s00335-005-0011-5. PubMed PMID:
524 16245023.
525 18. Eeken JC, de Jong AW, Loos M, Vreeken C, Romeyn R, Pastink A, et al. The nature of X-
526 ray-induced mutations in mature sperm and spermatogonial cells of Drosophila melanogaster.
527 Mutat Res. 1994;307(1):201-12. Epub 1994/05/01. doi: 10.1016/0027-5107(94)90293-3.
528 PubMed PMID: 7513798.
529 19. Pastink A, Vreeken C, Schalet AP, Eeken JC. DNA sequence analysis of X-ray-induced
530 deletions at the white locus of Drosophila melanogaster. Mutat Res. 1988;207(1):23-8. Epub
531 1988/01/01. doi: 10.1016/0165-7992(88)90006-1. PubMed PMID: 3122035.
532 20. Pastink A, Schalet AP, Vreeken C, Paradi E, Eeken JC. The nature of radiation-induced
533 mutations at the white locus of Drosophila melanogaster. Mutat Res. 1987;177(1):101-15. Epub
534 1987/03/01. doi: 10.1016/0027-5107(87)90026-1. PubMed PMID: 2881201.
535 21. Martin-Blanco E, Gampel A, Ring J, Virdee K, Kirov N, Tolkovsky AM, et al. puckered
536 encodes a phosphatase that mediates a feedback loop regulating JNK activity during dorsal
537 closure in Drosophila. Genes Dev. 1998;12(4):557-70. Epub 1998/03/21. doi:
538 10.1101/gad.12.4.557. PubMed PMID: 9472024; PubMed Central PMCID: PMCPMC316530.
539 22. Lawrence PA, Sanson B, Vincent JP. Compartments, wingless and engrailed: patterning
540 the ventral epidermis of Drosophila embryos. Development. 1996;122(12):4095-103. Epub
541 1996/12/01. doi: 10.1242/dev.122.12.4095. PubMed PMID: 9012529.

542 23. Kerkis J. The Growth of the Gonads in DROSOPHILA MELANOGASTER. Genetics.
543 1931;16(3):212-24. Epub 1931/05/01. doi: 10.1093/genetics/16.3.212. PubMed PMID:
544 17246617; PubMed Central PMCID: PMCPMC1201094.
545 24. Charan J, Kantharia ND. How to calculate sample size in animal studies? J Pharmacol
546 Pharmacother. 2013;4(4):303-6. doi: 10.4103/0976-500X.119726. PubMed PMID: 24250214;
547 PubMed Central PMCID: PMCPMC3826013.
548

Figure 1

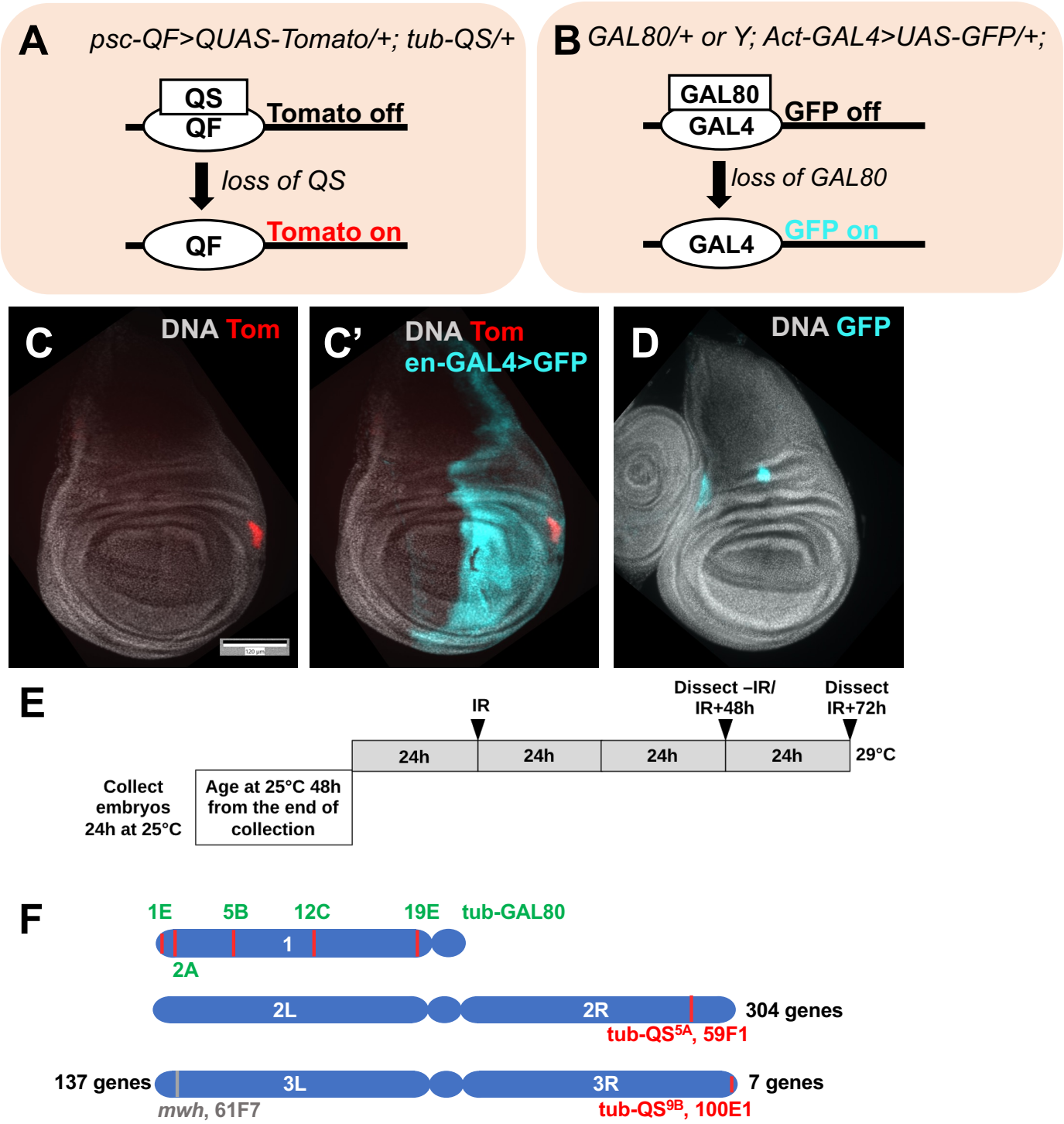
A
psc-QF>QUAS-Tomato/+; tub-QS/+
QS
QF
Tomato off
loss of QS
QF
Tomato on
B
GAL80/+ or Y; Act-GAL4>UAS-GFP/+;
GAL80
GAL4
GFP off
loss of GAL80
GAL4
GFP on
C
DNA Tom
C'
DNA Tom
en-GAL4>GFP
D
DNA GFP
E
IR
Dissect –IR/
IR+48h
Dissect
IR+72h
24h
24h
24h
24h
29°C
Collect
embryos
24h at 25°C
Age at 25°C 48h
from the end of
collection
F
1E
5B
12C
19E
tub-GAL80
1
2A
2L
2R
304 genes
tub-QS5A, 59F1
137 genes
3L
3R
7 genes
mwh, 61F7
tub-QS9B, 100E1

Figure 2

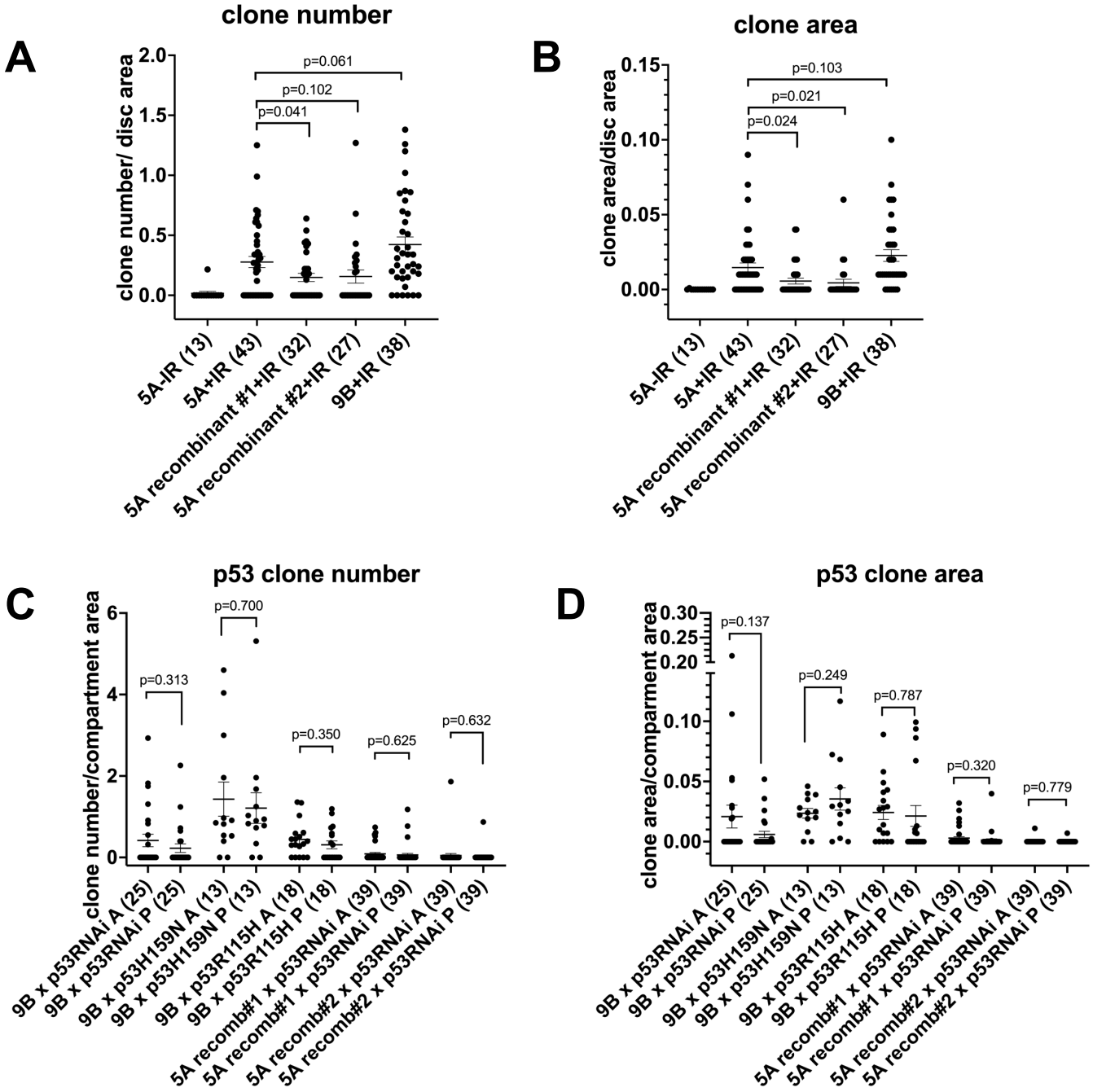
A
clone number
clone number/ disc area
2.0
1.5
1.0
0.5
0.0
p=0.061
p=0.102
p=0.041
5A-IR (13)
5A+IR (43)
5A recombinant #1+IR (32)
5A recombinant #2+IR (27)
9B+IR (38)
B
clone area
clone area/disc area
0.15
0.10
0.05
0.00
p=0.103
p=0.021
p=0.024
5A-IR (13)
5A+IR (43)
5A recombinant #1+IR (32)
5A recombinant #2+IR (27)
9B+IR (38)
C
p53 clone number
clone number/compartment area
6
4
2
0
p=0.313
p=0.700
p=0.350
p=0.625
p=0.632
9B x p53RNAi A (25)
9B x p53RNAi P (25)
9B x p53H159N A (13)
9B x p53H159N P (13)
9B x p53R115H A (18)
9B x p53R115H P (18)
5A recomb#1 x p53RNAi A (39)
5A recomb#1 x p53RNAi P (39)
5A recomb#2 x p53RNAi A (39)
5A recomb#2 x p53RNAi P (39)
D
p53 clone area
clone area/compartment area
0.30
0.25
0.20
0.10
0.05
0.00
p=0.137
p=0.249
p=0.787
p=0.320
p=0.779
9B x p53RNAi A (25)
9B x p53RNAi P (25)
9B x p53H159N A (13)
9B x p53H159N P (13)
9B x p53R115H A (18)
9B x p53R115H P (18)
5A recomb#1 x p53RNAi A (39)
5A recomb#1 x p53RNAi P (39)
5A recomb#2 x p53RNAi A (39)
5A recomb#2 x p53RNAi P (39)

Figure 3

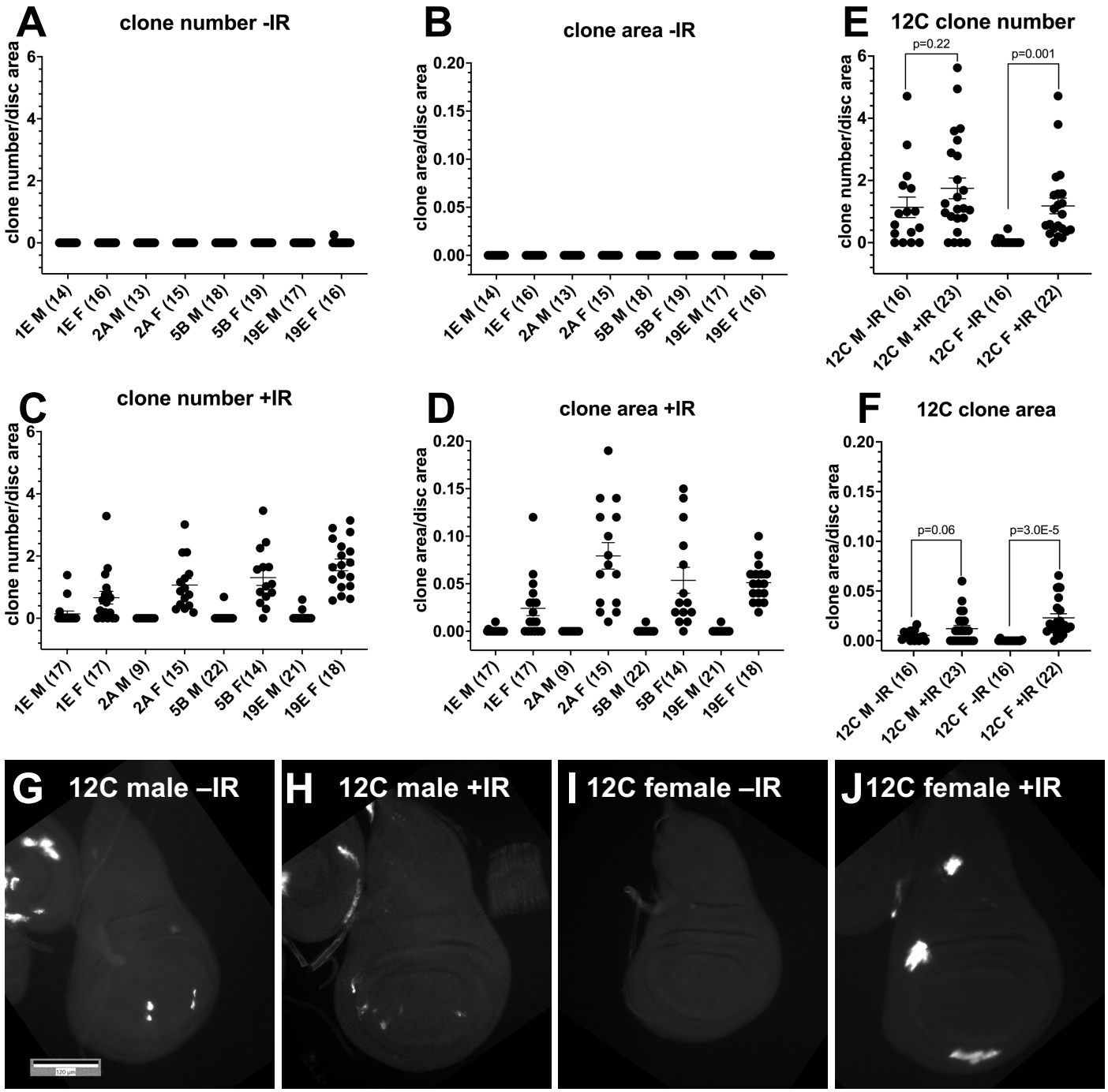
A
clone number -IR
clone number/disc area
1E M (14)
1E F (16)
2A M (13)
2A F (15)
5B M (18)
5B F (19)
19E M (17)
19E F (16)
B
clone area -IR
clone area/disc area
E
12C clone number
p=0.22
p=0.001
12C M -IR (16)
12C M +IR (23)
12C F -IR (16)
12C F +IR (22)
C
clone number +IR
1E M (17)
1E F (17)
2A M (9)
2A F (15)
5B M (22)
5B F(14)
19E M (21)
19E F (18)
D
clone area +IR
F
12C clone area
p=0.06
p=3.0E-5
G
12C male –IR
H
12C male +IR
I
12C female –IR
J
12C female +IR

Figure 4

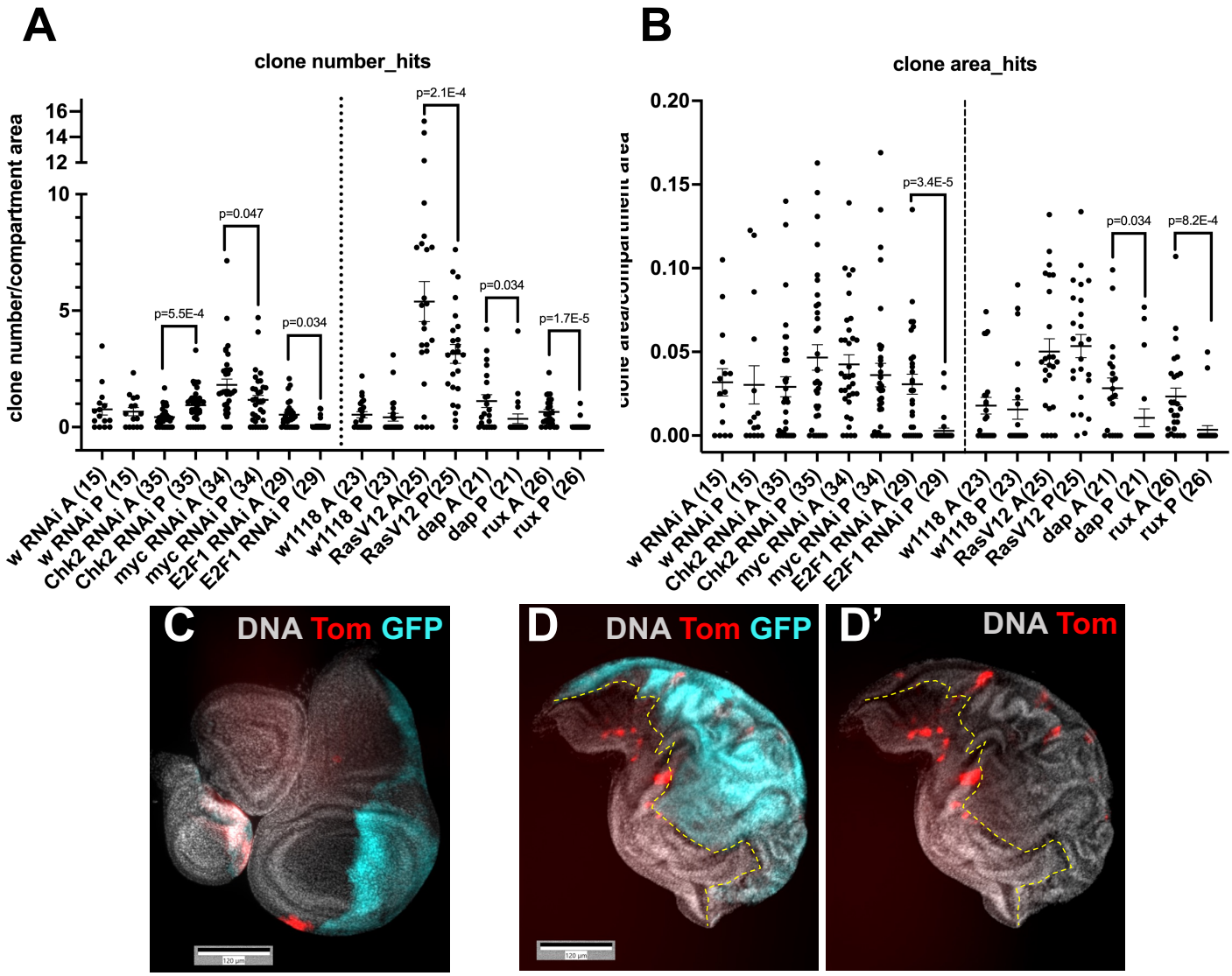

E2F1 RNAi

RAS^{V12}

Figure 5

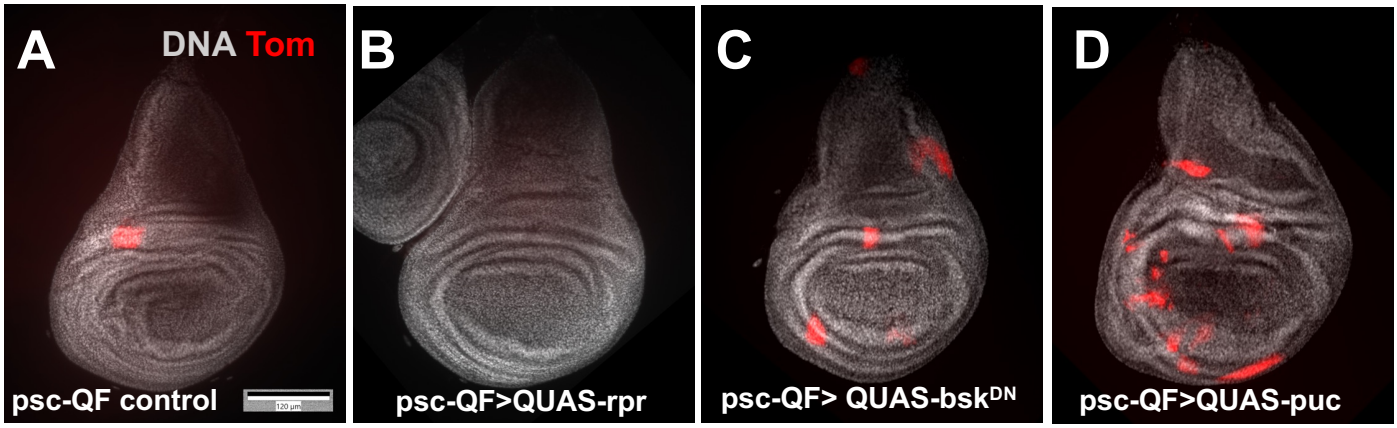
A
DNA Tom
psc-QF control
120 µm
B
psc-QF>QUAS-rpr
C
psc-QF> QUAS-bskDN
D
psc-QF>QUAS-puc

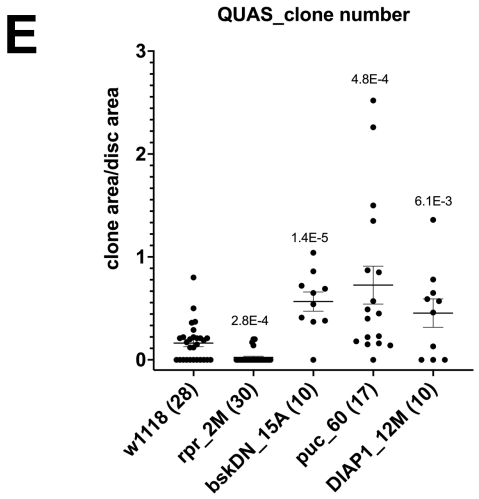
E
QUAS_clone number
clone area/disc area
0
1
2
3
2.8E-4
1.4E-5
4.8E-4
6.1E-3
w1118 (28)
rpr_2M (30)
bskDN_15A (10)
puc_60 (17)
DIAP1_12M (10)

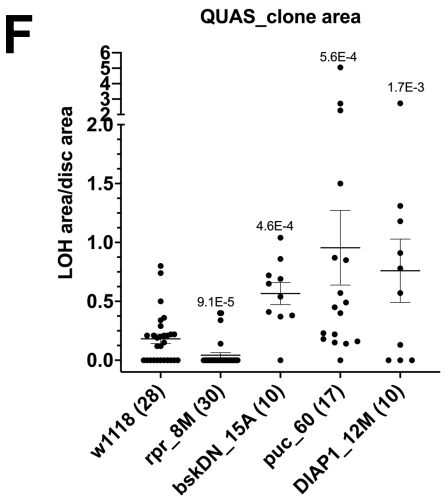
F
QUAS_clone area
LOH area/disc area
0.0
0.5
1.0
1.5
2.0
9.1E-5
4.6E-4
5.6E-4
1.7E-3
w1118 (28)
rpr_8M (30)
bskDN_15A (10)
puc_60 (17)
DIAP1_12M (10)

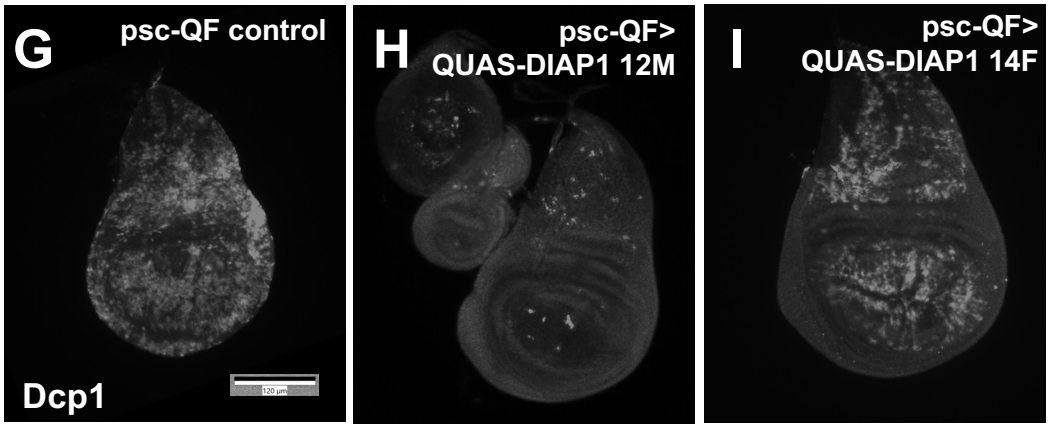
G
psc-QF control
Dcp1
120 µm
H
psc-QF>
QUAS-DIAP1 12M
I
psc-QF>
QUAS-DIAP1 14F

Supplemental Figure 1

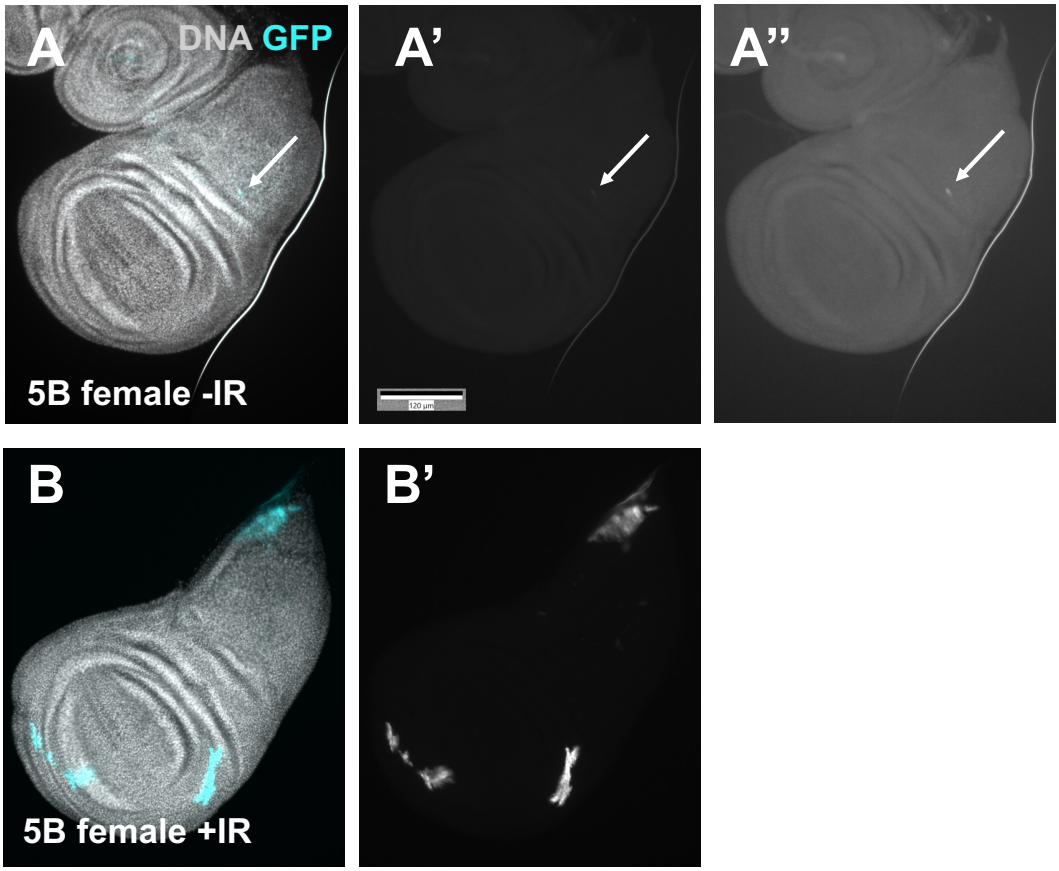

Supplemental Figure 1. Spontaneous GFP is less bright than IR-induced GFP.
Larvae were treated as in Fig 1E but without the temperature shift and wing discs were fixed and stained to visualize DNA. The genotype of the larvae was GAL80^{5B}/+; Act-GAL4, UAS-GFP/+ from the cross of GAL80^{5B}/GAL80^{5B} with Act-GAL4, UAS-GFP/CyO RFP Tb.

(A-A'''') A disc from an unirradiated larva showing one faint GFP spot (arrow).

(B-B') A disc from an irradiated larva showing bright GFP spots. A' and B' are shown with similar brightness and contrast range in ImageJ so that signals would be directly comparable. A'' is shown with a narrower range to allow the viewer to see the faint GFP spot.

Supplemental Figure 2

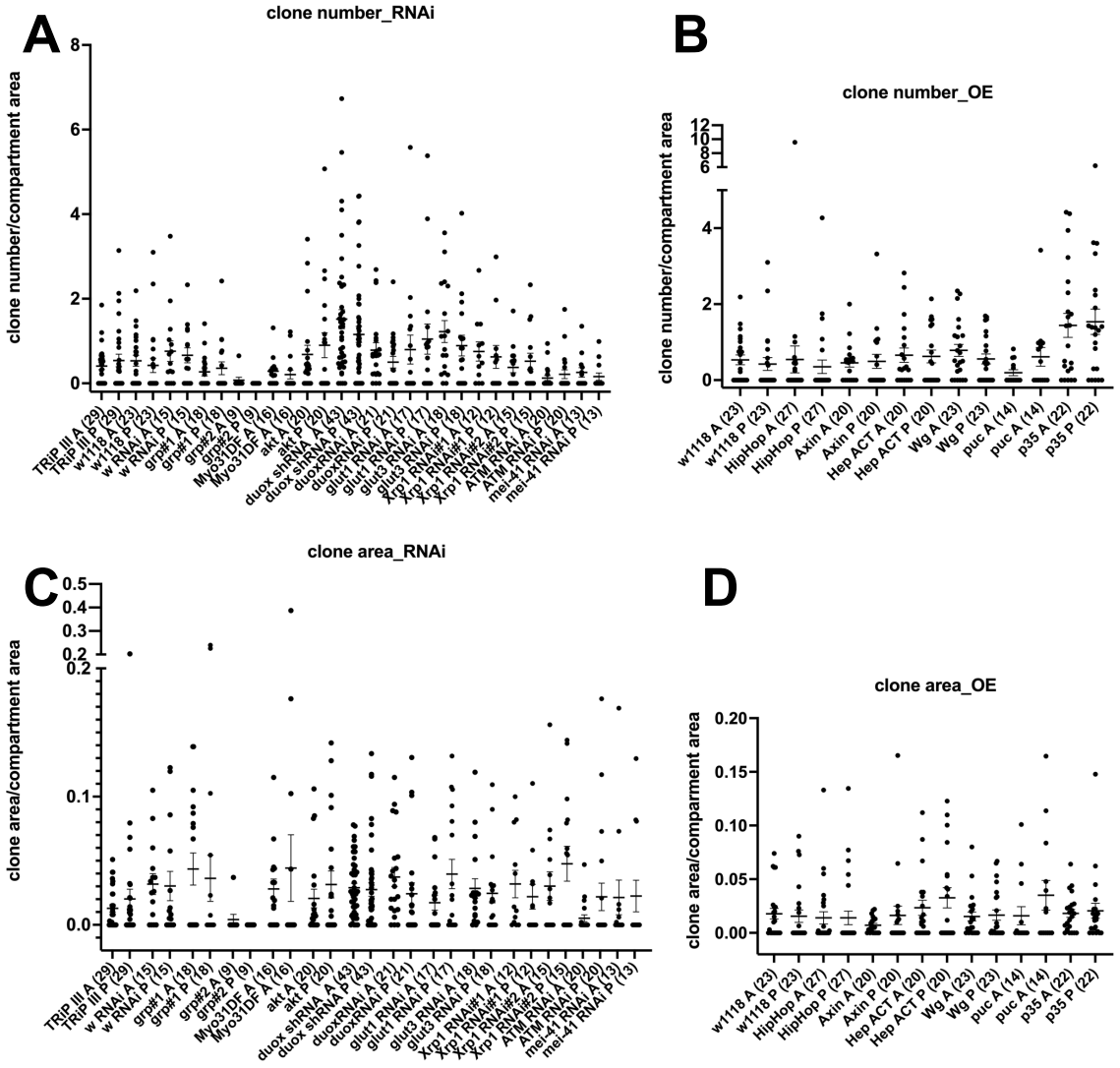

Supplemental Figure 2. A focused screen for modulators of IR-induced QS^{9B} LOH.
Wing discs from 3rd instar larvae were dissected 3 days after irradiation, fixed, and stained for DNA. Larvae were treated as in Fig 1E. The graphs show data from at least two biological replicates per sample, with the total number of wing discs examined per sample shown in parentheses. The mean±1 SEM is shown for each sample. Because A and P compartments are of different sizes, clone numbers and clone areas have been normalized to compartment area. p-values between A and P samples for each genotype (none <0.05) were calculated using a paired 2-tailed t-test. TRiP III (background stock for most RNAi lines used) and RNAi against w served as controls for RNAi constructs and w^{1118} served as the control for overexpression constructs.

(A-B) LOH clone numbers for RNAi (A) and overexpression (OE,B) constructs.

(C-D) LOH clone areas for RNAi (C) and overexpression (OE,D) constructs.

Supplemental Table 1

Supplemental Table 1. Drosophila stocks used in this work					
I. General stocks (BL = Bloomington Stock Center)					
stock #/source	*used in Fig.*	*used for*	*genotype*		
BL30042	Fig 2, 4, 5, S1	monitor LOH of QS{9B}	y[1] w[1118]; P{w[+mC]=M2ET-QF}ET40, P{w[+mC]=QUAS-mtdTomato-3xHA}CP; P{ry[+t7.2]=neoFRT}82B P{w[+mC]=tub-QS.P}9B		
BL30133	Fig 1, 2	monitor LOH of QS{5A}	y[1] w[1118]; P{w[+mW.hs]=FRT(w[hs])}G13 P{w[+mC]=tub-QS.P}5A		
BL30043	Fig 2, 4, 5, S1, Table S2	expresses Tom throughout the wing disc	y[1] w[1118]; P{w[+mC]=QUAS-mtdTomato-3xHA}14 P{w[+mC]=M2ET-QF}ET40/CyO		
BL24645	Fig 2	enhance p53 RNAi	P{w[+mC]=UAS-Dcr-2.D}1, w[1118]; Df(3L)Ly, sens[Ly-1]/TM3, Sb[1]		
unknown	Fig 1, 2, 4, S1	P compartment expression	engrailed-GAL4 on chromosome II		
BL5431	Fig 1, 2, 4, S1	mark the P compartment	UAS-eGFP on chromosome II		
Bardin lab	Fig 3	detecting loss of GAL80	Actin-GAL4, UAS-GFP		
II. Stocks used in the focused screen and for functional testing (VDRC = Vienna Drosophila Resource Center)					
gene	*function*	*construct*	*manipulation*	*stock #*	*ref./source*
p35	anti-apoptotic	UAS-p35	overexpression	BL5073	Bloomington Stock Center
Diap1	anti-apoptotic	QUAS-DIAP1	overexpression	N/A	Steller lab
p53	pro-apoptotic	UAS-dsRNA	RNAi	V38235	VDRC
p53	pro-apoptotic	UAS-p53R115H	dominant negative	BL8419	Bloomington Stock Center, ref.9
p53	pro-apoptotic	UAS-p53H159N	dominant negative	BL8421	Bloomington Stock Center, ref.9
rpr	pro-apoptotic	QUAS-rpr	overexpression	N/A	Steller lab, ref.14
E2F1	cell cycle, apoptosis	UAS-dsRNA	RNAi	BL27564	Bloomington Stock Center
rux	inhibits mitotic Cdk	UAS-Rux	overexpression	BL9166	Bloomington Stock Center
dap	inhibits G1/S Cdk	UAS-Dap	overexpression	BL83334	Bloomington Stock Center
tefu/ATM	DNA damage response	UAS-dsRNA	RNAi	V22502	VDRC
mei-41/ATR	DNA damage response	UAS-dsRNA	RNAi	v11251	VDRC
grp/Chk1	DNA damage response	UAS-dsRNA	RNAi (GL00067)	N/A	Perrimon lab
grp/Chk1#2	DNA damage response	UAS-dsRNA	RNAi (HMS01573)	BL36685	Bloomington Stock Center
loki/Chk2	DNA damage response	UAS-dsRNA	RNAi	BL35152	Bloomington Stock Center
hiphop	chromosome end protection	P{EPgy2} insertion	overexpression (with GAL4)	BL17618	Bloomington Stock Center
Puc	represses JNK signaling	UAS-puc	overexpression	N/A	ref.21
Puc	represses JNK signaling	QUAS-puc	overexpression	N/A	Steller lab
Bsk/JNK	stress response	QUAS-JNK DN	dominant negative	N/A	Steller lab
hep/JNKK	Stress response	UAS-hep ACT	constitutively active	BL9306	Bloomington Stock Center
Akt	Stress response	UAS-dsRNA	RNAi	BL31701	Bloomington Stock Center
myc	Growth	UAS-dsRNA	RNAi	v2947	VDRC
Ras	Growth, apoptosis	UAS-RAS V12 mutant	constitutively active	BL64195	Bloomington Stock Center
wg/Wnt1	Developmental signaling	UAS	overexpression	N/A	ref.22
Axin	inhibits Wg signaling	UAS-Axin	overexpression	BL7225	Bloomington Stock Center
duox	Cell competition	UAS-dsRNA	RNAi	BL33975	Bloomington Stock Center
duox	Cell competition	UAS-shRNA	shRNA	v330085	VDRC
Myo31DF	Cell competition	UAS-dsRNA	RNAi	BL33971	Bloomington Stock Center
Xrp1	Cell competition	UAS-dsRNA	RNAi	v107860	VDRC
glut1	p53 target	UAS-dsRNA	RNAi	v13326	VDRC
glut3	p53 target	UAS-dsRNA	RNAi	v13302	VDRC
w	control	UAS-dsRNA	RNAi	BL33623	Bloomington Stock Center
TRiP III	control stock for RNAi lines	N/A	none	BL36303	Bloomington Stock Center
w1118	control	none	none	BL3605	Bloomington Stock Center

Supplemental Table 2

Supplemental Table 2. X2 test for survival after ubiquitous expression of QUAS transgenes.													
Psc-QF, mtdTomato/CyO-GFP virgins crossed to	tested stock (stock#)	inserted Chromosome	Cy	Cy+	GFP-	GFP+	total	expected Cy or GFP-	expected Cy+ or GFP-	(o-e)^2	(o-e)^2	X2	p
N/A	**w1118 control**		**38**	**50**			**88**	**44**	**44**	**36.0**	**36.0**	**1.6**	**n.s.**
QUAS-X/CyO; Sb/TM6 Tb	QUAS-rpr (11M)	2	88	0	N/A	N/A	88	44	44	1936.0	1936.0	88.0	<0.001
QUAS-X/CyO; Sb/TM6 Tb	QUAS-rpr (12M)	2	58	0	N/A	N/A	58	29	29	841.0	841.0	58.0	<0.001
Sco/CyO; QUAS-X/TM6 Tb	**QUAS-rpr (2M)**	**3**	**N/A**	**N/A**	**0**	**47**	**47**	**31**	**16**	**981.8**	**981.8**	**94.0**	**<0.001**
QUAS-X/CyO; Sb/TM6 Tb	QUAS-DIAP1 (3M)	2	34	14	N/A	N/A	48	24	24	100.0	100.0	8.3	<0.005
QUAS-X/CyO; Sb/TM6 Tb	QUAS-DIAP1 (8M)	2	64	24	N/A	N/A	88	44	44	400.0	400.0	18.2	<0.001
QUAS-X/CyO; Sb/TM6 Tb	**QUAS-DIAP1 (12M)**	**2**	**49**	**61**	**N/A**	**N/A**	**110**	**55**	**55**	**36.0**	**36.0**	**1.3**	**n.s.**
QUAS-X/CyO; Sb/TM6 Tb	QUAS-bskDN (19)	2	38	0	N/A	N/A	38	19	19	361.0	361.0	38.0	<0.001
Sco/CyO; QUAS-X/TM6 Tb	**QUAS-bskDN (15A)***	**3**	**N/A**	**N/A**	**0**	**25**	**25**	**17**	**8**	**277.8**	**277.8**	**50.0**	**<0.001**
Sco/CyO; QUAS-X/TM6 Tb	QUAS-bskDN (30)	3	N/A	N/A	4	19	23	15	8	128.4	128.4	25.1	<0.001
Sco/CyO; QUAS-X/TM6 Tb	QUAS-bskDN (43)	3	N/A	N/A	2	13	15	10	5	64.0	64.0	19.2	<0.001
QUAS-X/CyO; Sb/TM6 Tb	QUAS-puc (21)	2	30	0	N/A	N/A	30	15	15	225.0	225.0	30.0	<0.001
QUAS-X/CyO; Sb/TM6 Tb	QUAS-puc (66)	2	72	10	N/A	N/A	82	41	41	961.0	961.0	46.9	<0.001
Sco/CyO; QUAS-X/TM6 Tb	QUAS-puc (59)	3	N/A	N/A	0	12	12	8	4	64.0	64.0	24.0	<0.001
Sco/CyO; QUAS-X/TM6 Tb	**QUAS-puc (60)**	**3**	**N/A**	**N/A**	**0**	**16**	**16**	**11**	**5**	**113.8**	**113.8**	**32.0**	**<0.001**
*counted as pupa													